Damage evaluation of craniofacial localized scleroderma using magnetic resonance imaging

Xuda Ma[1]#, Jiuzuo Huang[1]#, Huadan Xue[2], Hongwei Wang[3], Tianjiao Wang[2], Yu Chen[2], Xiao Long[1], Xiaojun Wang[1]

[1]Department of Plastic Surgery, Peking Union Medical College Hospital, Peking Union Medical College and Chinese Academy of Medical Sciences, Beijing, China; [2]Department of Radiology, Peking Union Medical College Hospital, Peking Union Medical College and Chinese Academy of Medical Sciences, Beijing, China; [3]Department of Dermatology, Peking Union Medical College Hospital, Peking Union Medical College and Chinese Academy of Medical Sciences, Beijing, China

Contributions: (I) Conception and design: X Ma, J Huang, H Wang, Y Chen, X Long, X Wang; (II) Administrative support: Y Chen, H Xue, X Long, X Wang; (III) Provision of study materials or patients: X Ma, J Huang, X Long, X Wang; (IV) Collection and assembly of data: X Ma, J Huang, T Wang, Y Chen; (V) Data analysis and interpretation: X Ma, J Huang, T Wang, Y Chen, X Long; (VI) Manuscript writing: All authors; (VII) Final approval of manuscript: All authors.

#These authors contributed equally to this work.

Correspondence to: Yu Chen, MD. Department of Radiology, Peking Union Medical College Hospital, Peking Union Medical College and Chinese Academy of Medical Sciences, No. 1 Shuaifuyuan, Wangfujing, Dongcheng District, Beijing 100730, China. Email: bjchenyu@126.com; Xiao Long, MD; Xiaojun Wang, MD. Department of Plastic Surgery, Peking Union Medical College Hospital, Peking Union Medical College and Chinese Academy of Medical Sciences, No. 1 Shuaifuyuan, Wangfujing, Dongcheng District, Beijing 100730, China. Email: pumclongxiao@126.com; pumchwxj@163.com.

Background: Localized scleroderma (LoS) is an autoimmune disease in which craniofacial lesions can cause severe facial deformities with brain involvement. Objective evaluation of craniofacial LoS is challenging. Magnetic resonance imaging (MRI) may be used as a damage assessment tool. This study aimed to analyze the tissue involvement of craniofacial LoS based on MRI and evaluate MRI for craniofacial LoS assessment.

Methods: This cross-sectional study included patients with craniofacial LoS from September 2021 to August 2022 in Peking Union Medical College Hospital. Patients who were clinically assessed in a stable phase were enrolled; patients with previous surgical treatment or contraindications to MRI were excluded. Participants underwent clinical, MRI, and ultrasound assessments. MRI was compared with ultrasound by correlation analysis and Bland-Altman analysis. The involvement of different tissues and different facial subunits was compared. The accumulated soft tissue atrophy index (ASTAI) was compared with clinical scores by correlation analysis.

Results: A total of 28 patients were included (13 female; mean age, 18 years). MRI showed a good correlation and agreement with ultrasound (r=0.916, P<0.001). In different facial subunits, a significant negative correlation between the forehead and chin was found (r=−0.593, P=0.001). The ASTAI correlated well with the facial LoS damage index (r=0.580, P=0.001) and the Peking Union Medical College LoS facial aesthetic index (PUMC LoSFAI) (r=0.921, P<0.001). A total of 38.6% of clinical scores were inaccurate based on MRI. Neurological changes were found in one patient.

Conclusions: MRI can reliably quantify damage in craniofacial LoS, and may serve as a useful and objective tool for overall craniofacial LoS evaluation.

Keywords: Localized scleroderma (LoS); craniofacial morphea; magnetic resonance imaging (MRI); en coup de sabre (ECDS); Parry-Romberg syndrome (PRS)

Introduction

Localized scleroderma (LoS) is a rare acquired autoimmune disorder characterized by inflammation, sclerosis and atrophy of the skin and underlying tissue (1). Unlike in systemic sclerosis (SSc), the skin and subcutaneous soft tissue are affected in most instances of LoS, while visceral involvement is absent. Although it is considered relatively benign in most cases, LoS can cause severe deep damage, especially in the craniofacial region (2).

Craniofacial LoS can involve the skin, subcutaneous fat, facial muscles, bones and brain, which leads to different degrees of cosmetic damage and sometimes even functional disorders (2-5). En coup de sabre (ECDS) and Parry-Romberg syndrome (PRS, also known as progressive hemifacial atrophy) are two typical and indistinguishable forms of craniofacial LoS. Regardless of the form, craniofacial LoS occurs unilaterally in most cases. The precise and thorough evaluation of activity and damage is the premise of disease management. Numerous methods have been applied in condition evaluation and monitoring, such as the Localized Scleroderma Cutaneous Assessment Tool (LoSCAT) (6,7), traditional or three dimensional (3D) photography (8,9), infrared thermography (10), laboratory tests (11), ultrasonography (12-14), and magnetic resonance imaging (MRI) (4,15-17). Considering the particularity of the craniofacial region, specific methods are needed for evaluation (4,9,17). Previously, we developed a clinical scoring system called the Peking Union Medical College LoS facial aesthetic index (PUMC LoSFAI) for LoS aesthetic impairment (18). Nevertheless, there is a lack of a comprehensive and objective craniofacial LoS assessment method, and current methods are insufficient for deep tissue assessment.

MRI may detect underlying neurological involvement and is recommended for evaluation by the Single Hub and Access point for pediatric Rheumatology in Europe (19) and the European Dermatology Forum S1-guideline (20). However, the information provided by MRI in the craniofacial region beyond central nervous system (CNS) involvement is often ignored in making diagnoses.

In this study, we performed a quantitative assessment of craniofacial LoS based on MRI, explored its clinical significance by comparing it with ultrasound and clinical assessments, and explored the disease characteristics in different facial subunits at different levels. We present this article in accordance with the STROBE reporting checklist (available at https://qims.amegroups.com/article/view/10.21037/qims-23-980/rc).

Methods

Patients and clinical assessment

This cross-sectional study was approved by the institutional review board of Peking Union Medical College Hospital (No. I-22PJ352) following the Declaration of Helsinki (as revised in 2013). All patients or the legal guardians for adolescent patients provided written informed consent for the study procedures, which included MRI scans, ultrasonography and photography. A total of 28 patients were included from September 2021 to August 2022 (*Figure 1*), and all patients were diagnosed with LoS and classified according to the Padua criteria by dermatologists (21). Patients who were in the active phase and had undergone previous surgical treatment were excluded. Patients who could not undergo MRI were also excluded. In this study, linear scleroderma of the head (ECDS and PRS) and other types of morphea located on the head were considered as craniofacial LoS. All patients underwent long-term treatment at our hospital and were clinically judged to be stationary by a multidisciplinary team consisting of dermatologists, plastic surgeons and radiologists. After careful clinical evaluation, the patients were rated using the LoSCAT, which includes the modified LoS severity index (mLoSSI) and LoS Damage Index (LoSDI). The PUMC LoSFAI, based on both local and overall assessment, was used for detailed damage assessment. No active changes were found on ultrasound (12) or MRI (15).

MRI scan protocols

MRI was performed using a 3.0 T (MAGNETOM Vida, Siemens Healthineers, Erlangen, Germany). The 3D Dixon T1W imaging was obtained with a gradient echo sequence (GRE). The acquisition voxel and reconstruction voxel were 1.14 mm/1.14 mm/1.00 mm. The fat, in-phase, opposed-phase, and water images were obtained by 3D Dixon T1-weighted (T1W) sequences. Transverse, sagittal and coronal

images were reconstructed from this 3D T1W image for 3D rendering and measurements as previously described (22). The regular 2D T1W and T2-weighted (T2W) Dixon turbo spin echo (TSE) with transverse orientation were also applied for CNS evaluation (the whole scan duration: 10 minutes). After the examination, the DICOM data were exported and adjusted again to confirm that the orientation of the axial image was parallel to the Frankfurt plane (*Figure 2*). The measurements and adjustments of the data were performed in 3D SLICER software version 5.0.3 (www.slicer.org) for Windows (23). Image evaluation

was performed in collaboration by a radiologist specialized in craniofacial MRI and a plastic surgeon specialized in LoS (both with over 10 years of work experience). In cases of persistent disagreement, a senior plastic surgeon participated in the discussion and unified the conclusion. *Figures 3,4* provide examples of MRI measurements of two patients with facial involvement mainly in the upper-middle and middle-lower areas.

Soft tissue assessment

For the assessments of skin and subcutaneous soft tissue, the facial surface was divided into six subunits, including the forehead, temporal, periocular, cheek, nose, and chin (18). The full-thickness soft tissue was measured on the affected side of the most severe axial section and the contralateral side. Due to the irregular shape of the nose, the most severely involved soft tissue on the surface of the nasal bone was measured. For patients with cheek involvement, the thicknesses of the masseter muscle were measured at the plane over the anterior nasal spine. For patients with temporal involvement, the temporalis muscle thicknesses were measured at the level of the orbital roof (24) (*Figure 3*).

The atrophy index was used to express the involvement relative to the unaffected side for different soft tissue comparisons: Ind. = (N − D)/N (Ind.: index of atrophy, N: normal side, D: disease side).

The soft tissue atrophy assessments by the LoSDI and PUMC LoSFAI were divided into four grades: grade 0 for no loss, 1 for mild loss, 2 for moderate loss, and 3 for severe
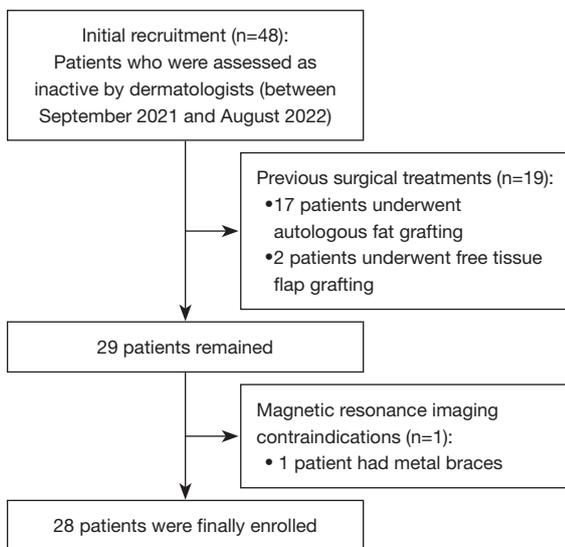

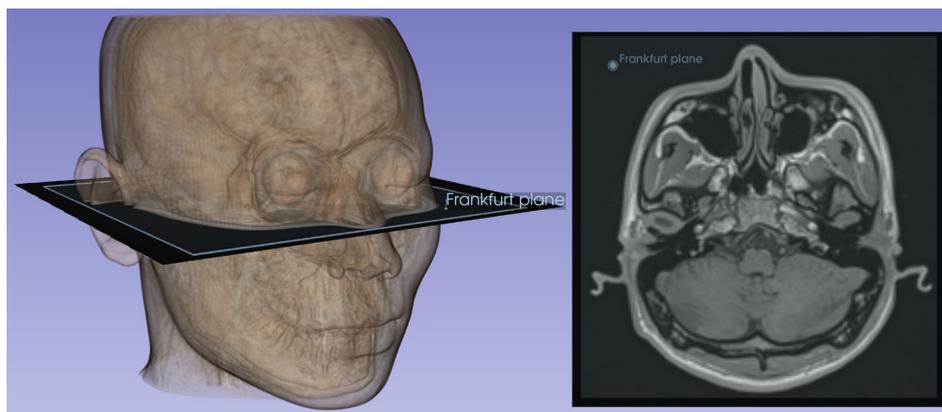
Figure 1 Flow diagram of patient enrollment.

Figure 2 Illustration of MRI measurements. This figure shows the MRI measurement of a 16-year-old male patient with craniofacial LoS, which mainly affected the upper and middle face. The images were calibrated according to the Frankfurt plane before starting the measurement by comparison with the 3D rendering model. MRI, magnetic resonance imaging; LoS, localized scleroderma; 3D, three dimensional.
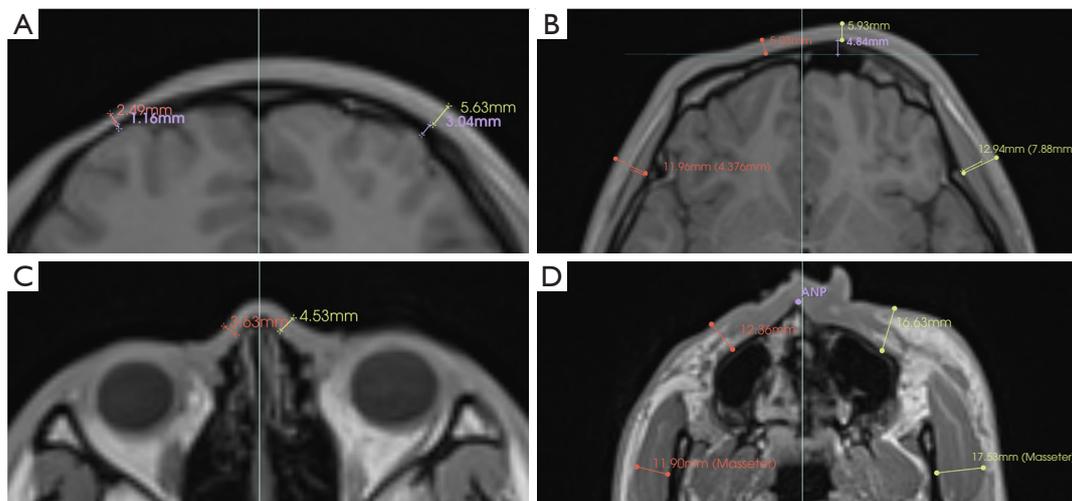
Figure 3 Illustration of MRI measurements of the upper and middle face. This figure shows the MRI measurement of the patient in *Figure 2*. Total soft tissue thickness of the most affected side (red) and normal side (yellow) was measured symmetrically in the forehead (A), periocular (B), temporal (B), nose (C) and cheek (D) subunit. The thicknesses of the masseter (D) and temporalis (B) muscles were measured in patients with cheek and temporal involvement. For bony structures, the thickness of the frontal bone was measured at the most affected and contralateral positions (purple in A). The retraction of the supraorbital ridge was measured at the most prominent and contralateral affected point (purple in B). ANP, anterior nasal spine; MRI, magnetic resonance imaging.
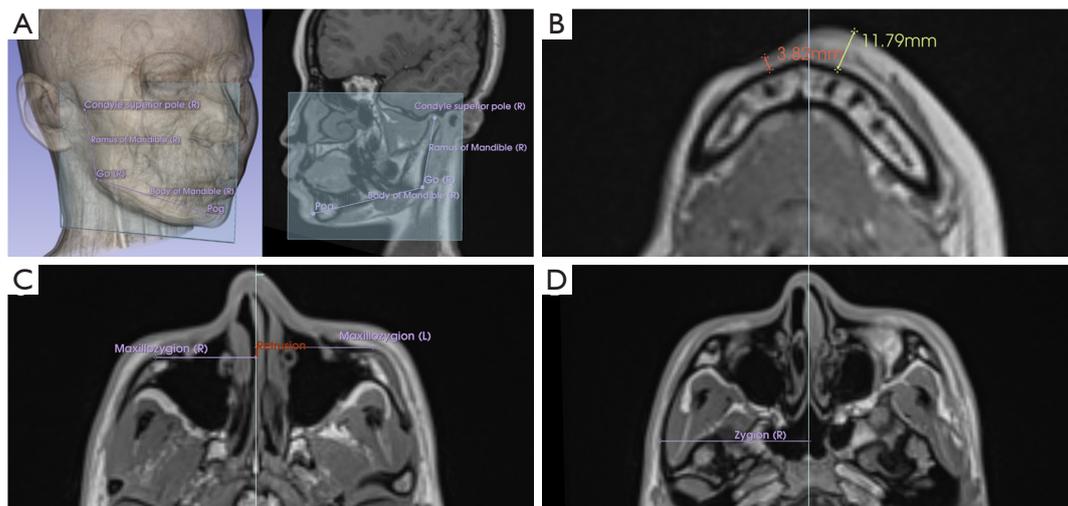

Figure 4 Illustration of MRI measurements of the middle and lower face. This figure shows the MRI measurement of a 14-year-old female patient with craniofacial LoS that mainly affected the middle and lower face. Bilateral mandibular ramus and body measurements were performed in the 3D model after positioning the pogonions, gonions and condyle superior poles on the affected and healthy sides (A). Total soft tissue thickness of the chin was measured at the most affected level (B). The inward and posterior shift of maxillozygions was measured by comparing the affected and normal sides (C), as well as the inward shift of zygions (D). Go, Gonion; Pog, Pogonion; MRI, magnetic resonance imaging; LoS, localized scleroderma; 3D, three dimensional.

Table 1 Anatomy landmarks for MRI and ultrasound measurements and descriptions

Measurement	Anatomy landmarks	Description
MRI	ANP	The most anterior point of lower margin of the anterior nasal opening
	Zygion	The most lateral point on the zygomatic arch
	Maxillozygion	The most prominent point on the frontal aspect of the face below the bony orbit
	Pog	The most anterior point on the contour of the mandible
	Go	The most inferior, posterior, and lateral point on the angle of the mandible
	Condyle superior pole	The most superior point of mandible condyle
Ultrasound	Frontal eminence	The most anterior point of the forehead (centered on eyepupil)
	Inferior malar	Centered on the eyepupil, just under the zygomatic process
	Mental tubercle anterior	The most prominent point on the lateral bulge of the chin mound

MRI, magnetic resonance imaging; ANP, anterior nasal spine; Pog, Pogonion; Go, Gonion.

loss. For comparison, MRI assessments were also divided into four grades: 0 (Ind. =0), 1 (Ind. <0.333), 2 (0.333< Ind. <0.666), 3 (Ind. >0.666) (7,18).

Bony structure assessment

On the upper face, the thickness measurements of the frontal bone at the most affected and contralateral sites were compared for patients with forehead involvement. The retraction of the supraorbital ridge was measured at the most prominent point. On the midface, the difference in the distance of the maxillozygion from the midline and the degree of posterior displacement was measured to assess zygomaticomaxillary complex involvement. Differences between the distance of the bilateral zygion relative to the midline were used to assess atrophy of the affected side of the zygomatic arch (25). The difference in the distance from the pogonion to the gonion bilaterally reflected atrophy of the mandibular body length, and the distance from the gonion to the condyle superior pole represented atrophy of the mandibular ramus length (26) (*Figure 4*). The anatomical landmarks and detailed discerptions are listed in *Table 1*.

Ultrasonography assessment

An ultrasound assessment was performed on 17 patients (cumulative total of 26 sites) on the forehead, cheek or chin (E-cube 7, Alpinion, with a 17H transductor, Seoul, Korea). Referring to a previous similar ultrasound study (13), the frontal, cheek, and chin involvement was measured (*Figure 5A*). Since these fixed points were not necessarily

the most severely affected areas, the most severely affected areas of the lesion on the horizontal line over the fixed points were used for the measurements, and the atrophy index was used for comparison. The anatomical landmarks are listed in *Table 1*. MRI measurements took 5–15 minutes and ultrasound measurements take 2–5 minutes per patient, depending on the extent of lesion.

Statistics

All measurements by MRI and ultrasound were assessed in triplicate independently by three experienced physicians, and the mean was used for analysis. Intraclass correlation coefficients (ICC) were calculated to estimate the reliability of the three different researchers (inter-rater ICC). The same measurements were repeated one week later, and ICC (intra-rater ICC) of means were also calculated for test-retest reliability. The clinical data were summarized using descriptive statistics. Correlation analyses and matrices were conducted using Pearson correlation coefficients (r). The Bland-Altman analysis was used to test the difference between MRI and ultrasound measurements. In the correlation matrix, the atrophy indices were defaulted to 0 for uninvolved subunits, and r was shown only in the results where there was a significant correlation. The cumulative bar chart was arranged in increasing order, with the horizontal axis indicating the patient ID number (e.g., P01 for patient number 01). There were no missing data. A value of $P<0.05$ was considered statistically significant for all tests (two-sided). All statistical tests were conducted in R version 4.1.1 (https://www.R-project.org/) for Windows, R
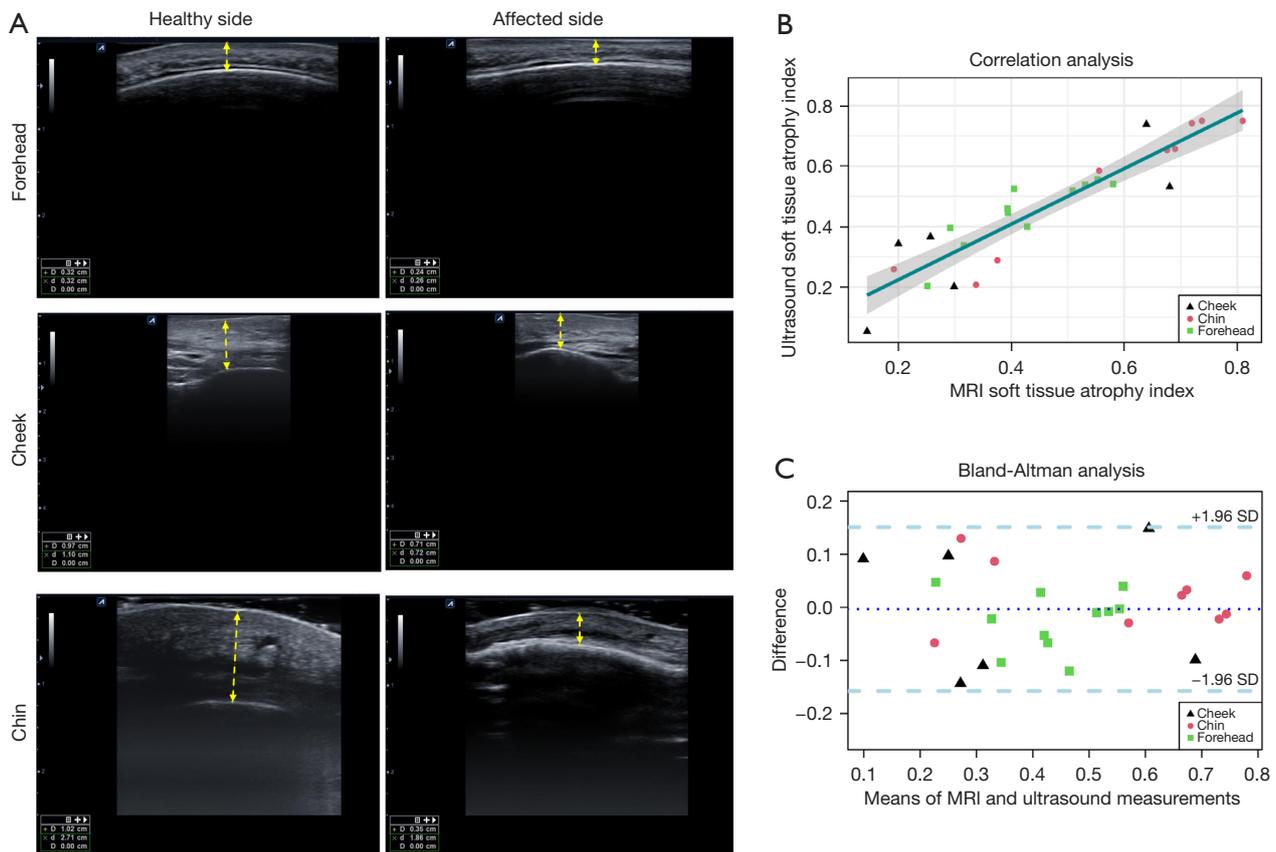
Figure 5 Comparison of ultrasound and MRI for soft tissue assessment. The ultrasound measurements of the forehead, cheek, and chin was shown (A). Yellow arrows indicate soft tissue thickness. There was a significant correlation between MRI- and ultrasound-based atrophy indices (B). The Bland-Altman analysis showed good agreement between MRI and ultrasound measurements (C). MRI, magnetic resonance imaging; cm, centimeter; SD, standard deviation.

Core Team [2021], Vienna, Austria.

Results

Patient information

Between September 2021 and August 2022, 48 patients were initially evaluated by dermatologists as being in the stable phase, of whom 17 had previous autologous fat grafting treatments, two had previous free tissue flap treatments, and one had metal braces, and 28 patients with inactive craniofacial LoS were finally enrolled (*Figure 1*). The majority had a pediatric onset (82.1%). The median (P25, P75) age of all patients was 18 (15.25, 23.25) years old. The proportion of male patients (n=15, 53.6%) was slightly higher than that of female patients (n=13, 46.4%). ECDS (n=15, 53.6%) was the most common subtype. The clinical scores and additional characteristics are presented in *Table 2*.

Comparison between MRI and ultrasound

To our knowledge, there were no previous studies related to MRI measurement of craniofacial LoS, but ultrasound is widely used for the measurement of facial LoS (13); therefore, ultrasound was used for comparison. Both MRI and ultrasound measurements showed good inter-rater reliability [ICC =0.873, 95% confidence interval (CI): 0.823–0.923; ICC =0.783, 95% CI: 0.703–0.863, respectively] and intra-rater reliability (ICC =0.891, 95% CI: 0.831–0.951; ICC =0.792, 95% CI: 0.712–0.872, respectively). The soft tissue involvement indices measured by ultrasound and MRI were compared because it was difficult to ensure that the same location was captured. The results showed a significant correlation between the findings of 26 ultrasounds and MRI at the corresponding regions (r=0.916, P<0.001) (*Figure 5B*). MRI and ultrasound showed excellent agreement in Bland-Altman plot analysis.

Table 2 Demographic characteristics and clinical information of the 28 patients with craniofacial LoS

Characteristic	Value
Onset	
Juvenile onset	23 (82.1)
Adult onset	5 (17.9)
Age (years old)	
Total	18 [15.25, 23.25]
Juvenile onset	18 [15, 20]
Adult onset	34 [26.5, 37]
Sex	
Female	13 (46.4)
Male	15 (53.6)
Subtype	
En coup de sabre	15 (53.6)
Parry Romberg	8 (28.6)
Both	3 (10.7)
Neither	2 (7.1)
Extra-facial involvement	
Total	6 (21.4)
Extra-facial skin involvement	3 (10.7)
Epilepsy	2 (7.1)
SLE	1 (3.6)
Clinical scores	
LoSCAT	
mLoSSI	0
LoSDI	6 [4, 7]
Facial LoSDI	6 [4, 7]
PUMC LoSFAI	19 [11.25, 27.25]

This table provides the clinical and demographic information of the patients in the cohort. Data are presented as n (%) or median [P25, P75]. LoS, localized scleroderma; SLE, Systemic Lupus Erythematosus; LoSCAT, Localized Scleroderma Cutaneous Assessment Tool; mLoSSI, modified localized scleroderma severity index; LoSDI, Localized Scleroderma Damage Index; PUMC LoSFAI, Peking Union Medical College LoS facial aesthetic index; P25 & P75, 25th and 75th percentile.

The differences in mean variations were within ±1.96 SD (standard deviation) of the mean in all patients (*Figure 5C*).

Soft tissue involvement of facial subunits

Of the 28 patients, 21 (75%) patients had forehead area involvement, 10 (35.7%) patients had temporal involvement, 17 (60.7%) patients had involvement of the periocular area, 11 (39.3%) patients had cheek involvement, 16 (57.1%) patients had nasal involvement, and 13 (46.4%) patients had chin involvement. Compared to the MRI measurements, a total of 38.6% of clinical scores were inaccurate, with 26.1% of scores being overestimated and 12.5% of scores being underestimated (*Table 3*). For example, in cases with severe bony involvement, soft tissue involvement may have been overestimated. As shown in *Figure 6*, MRI showed the same degree of soft tissue involvement, but a higher clinical score was rated for P17 in the clinical evaluation.

A correlation matrix was constructed based on the atrophy index to explore the potential correlation between the degree of atrophy of different facial subunits (*Figure 7A*). The correlation analysis of the severity of different involvement sites revealed significant positive correlations between the forehead and periocular (r=0.517, P=0.005), temporal and cheek (r=0.744, P<0.001), periocular and nose (r=0.648, P<0.001), and cheek and chin (r=0.526, P=0.004) involvement and significant negative correlations between the forehead and chin (r=−0.593, P=0.001).

The soft tissue involvement indices of the six anatomical subunits were accumulated to represent the overall involvement [accumulated soft tissue atrophy index (ASTAI)] (*Figure 7B*). The ASTAIs of 28 patients were distributed from 0.2963–2.3972. For comparison, the values of the facial LoSDI were distributed from 3 to 9, and the values of the PUMC LoSFAI were distributed from 5 to 40. We correlated ASTAI with the facial LoSDI (r=0.580, P=0.001) as well as the PUMC LoSFAI (r=0.921, P<0.001) and found significant positive correlations for both (*Figure 8*).

Assessment of deep tissue

First, we compared the extent of full soft tissue involvement with muscle tissue involvement in both the temporal

1898

Ma et al. Damage evaluation of craniofacial morphea by MRI

Table 3 Comparison between soft tissue atrophy assessment by MRI and PUMC LoSFAI

Variables	Forehead (n=21)	Temporal (n=10)	Periocular (n=17)	Cheek (n=11)	Nose (n=16)	Chin (n=13)	Total (n=88)
Higher	9 (42.9)	2 (20.0)	2 (11.8)	8 (72.7)	2 (12.5)	0	23 (26.1)
Lower	2 (9.5)	0	4 (23.5)	0	1 (6.3)	4 (30.8)	11 (12.5)
Total	11 (52.4)	2 (20.0)	6 (35.3)	8 (72.7)	3 (18.8)	4 (30.8)	34 (38.6)

This table shows the comparison of MRI assessment and clinical evaluation of soft tissue atrophy in different facial subunits. Data are presented as n (%). Higher (lower): the soft tissue atrophy grade of clinical score is higher (or lower) than MRI assessment; Total: overall differences. MRI, magnetic resonance imaging; PUMC LoSFAI, Peking Union Medical College LoS facial aesthetic index.

Figure 6 MRI indicates similar cheek soft tissue involvement in two patients with different clinical assessments. This figure shows an example of two localized scleroderma patients (P22 and P17) with similar cheek atrophy index that have distinct zygomaticomaxillary bony involvements (inward shift of zygion: P22 =1.9 mm, P17 =5.7 mm; inward shift of maxillozygion: P22 =1.5 mm, P17 =4.8 mm; posterior shift of maxillozygion: P22 =3.2 mm, P17 =8.9 mm). The cheek involvement of P22 was rated as grade 2 by MRI (cheek atrophy index: 0.639) and grade 2 by PUMC LoSFAI. The cheek involvement of P17 was also rated as grade 2 by MRI (cheek atrophy index: 0.639) but grade 3 by PUMC LoSFAI (cheek atrophy index: 0.653). This image is published with the patient's consent (P22, adult) or the patient's legal guardian's consent (P17, adolescent). MRI, magnetic resonance imaging; mm, millimeter; PUMC LoSFAI, Peking Union Medical College LoS facial aesthetic index.
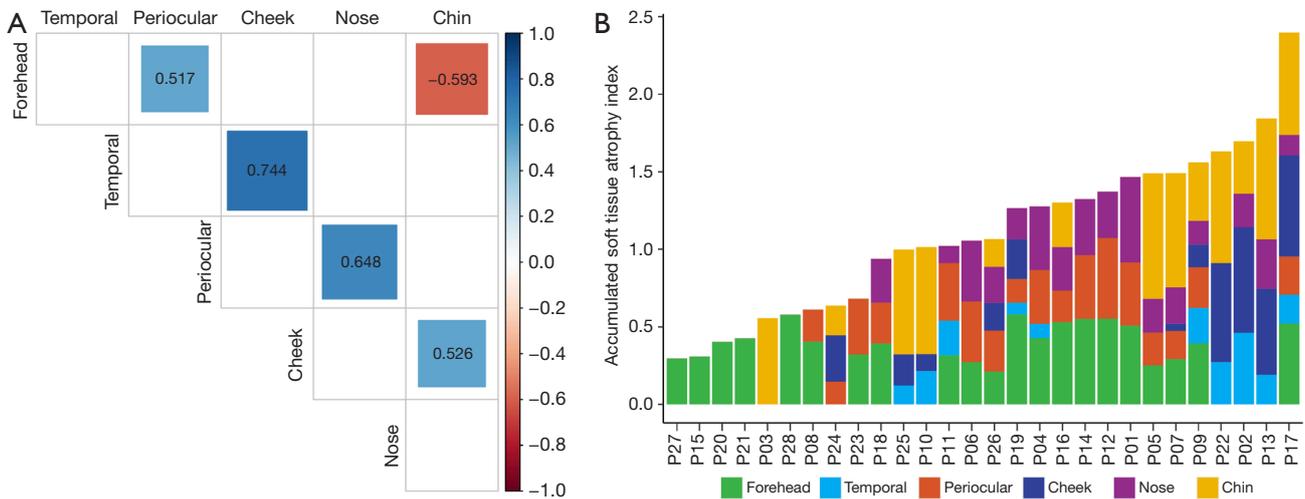
Figure 7 Analysis of the soft tissue atrophy index. This figure shows that the correlation matrix of the soft atrophy index revealed a negative correlation between forehead and chin involvement and a positive correlation between anatomically adjacent facial subunits (A). The ASTAI was derived by summing the atrophy indices of the six subunits of the face (B). ASTAI, accumulated soft tissue atrophy index.
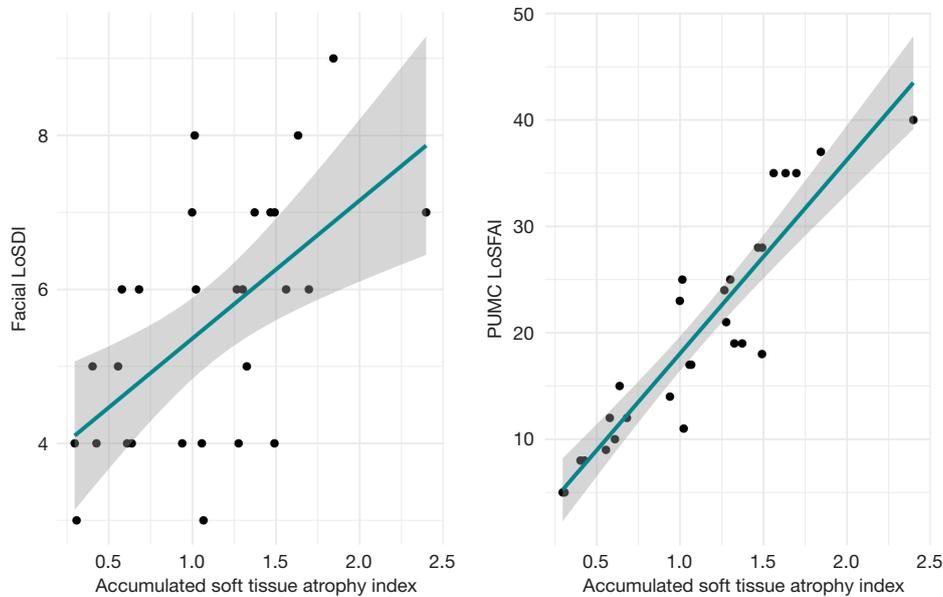

Figure 8 Comparison of ASTAI with LoSDI and PUMC LoSFAI. This figure shows that the ASTAI had significant positive correlations with facial LoSDI and PUMC LoSFAI. LoSDI, Localized Scleroderma Damage Index; PUMC LoSFAI, Peking Union Medical College LoS facial aesthetic index; ASTAI, accumulated soft tissue atrophy index.

(temporalis muscle) and cheek areas (masseter muscle). The results showed that there was no significant correlation between the total soft tissue atrophy and muscle atrophy. No significance was found in the analysis (*Figure 9*). The severity of the soft tissue involvement in different facial subunits was then compared with the corresponding bony alterations. Since the supraorbital ridge is at the junction of the forehead and the periauricular area, the correlation between the two areas was analyzed at the same time. The results showed that none of the changes in bony structures
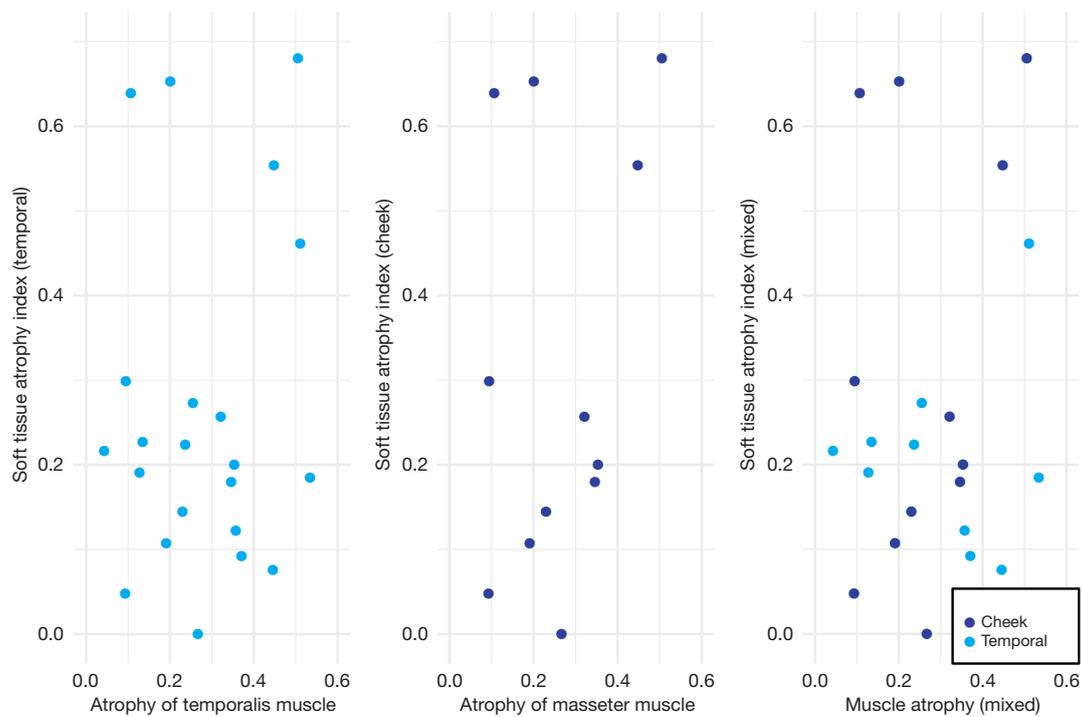
Figure 9 Comparison of soft tissue atrophy and muscle atrophy. Atrophy of the temporalis and masseter muscles does not correlate with the corresponding temporal and cheek regions.

were significantly correlated with the soft tissue atrophy indices at the corresponding sites (*Figure 10*). The bone tissue may vary greatly when the soft tissue involvement is similar (*Figure 6*). Zygomatic atrophy was significantly more severe in patient P17 than in patient P22.

CNS involvement is an assignable extracutaneous involvement of craniofacial LoS. In this study, two patients had a history of epilepsy; one was treated surgically, and the other improved with medication. None of the patients had headaches or migraines. No abnormalities were found, except for in the patient who had undergone surgical treatment, in which postoperative changes in the left cerebral hemisphere, absence of local structures of the left parietal lobe and temporal lobe, thinning of the temporal lobe gyrus, and expansion of the left lateral ventricle were observed.

Discussion

The purpose of this study was to perform an objective assessment of craniofacial LoS based on MRI. The results showed that MRI can accurately evaluate the damage in different facial subunits at different levels and may be used

as a new damage assessment method that is more accurate than clinical assessment. A more accurate assessment will help determine the damage and activity, thus providing a more accurate basis for the subsequent treatment. In addition to screening for brain lesions, regular MRIs can help determine if the damage has worsened and thus assist in determining whether the disease is stable or active.

To our knowledge, MRI has not been previously used for craniofacial LoS severity assessment. The four sets of images in the 3D Dixon sequence provided more information than the conventional head MRI. The in-phase and opposed-phase images showed clear soft tissue structures, and the borders of bone were easy to locate. Water images can detect potential inflammatory edema, and fat images can show subcutaneous fat alone, which is valuable for surgical repair, such as fat grafting (22). The application of MRI for craniofacial LoS assessment has some unique advantages over other objective evaluation methods (27). For example, computed tomography (CT) can provide a comprehensive assessment of bony structure involvement, but radiation limits its application. Ultrasound is convenient and economical. However, its consistency usually depends on the experience of the examiner. Although a combination
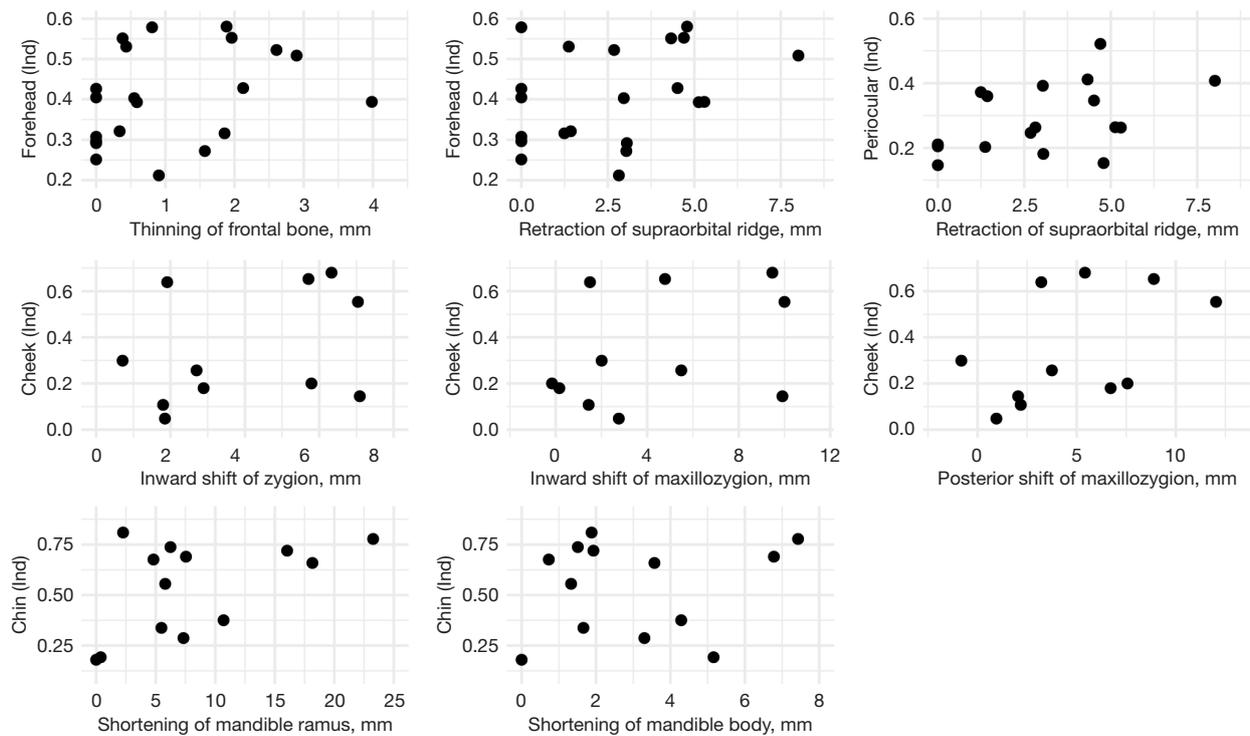
Figure 10 Comparison of soft tissue atrophy index and bony atrophy. No significant correlation was found between different facial subunits. Ind, index; mm, millimeter.

of examinations, such as CT with ultrasound, allows for a thorough and objective assessment, our results suggest that a single MRI scan allows for a simultaneous assessment of the face and the brain.

We analyzed the degree of atrophy of soft tissues in different facial subunits and verified that the ASTAI can be used as an objective analytical evaluation index for the severity of craniofacial LoS by comparing it with the facial LoSDI and PUMC LoSFAI. In particular, the PUMC LoSFAI had a high correlation coefficient (r=0.921, P<0.001), which may be caused by the same facial partition. However, 38.6% of the clinical assessments were inaccurate; for example, 72.7% of the cases in the cheek region were overestimated (*Table 3*). It is also worth noting that the values of the facial LoSDI in this study were concentrated between 3 and 9, which made it difficult to distinguish the severity.

The correlation analysis between the severity of the different subunits showed that the severity of precipitation in adjacent subunits was similar, while there was a significant negative correlation between the degree of involvement of the two most distant subunits, the forehead and the chin,

suggesting that there may be polarity in the soft tissue involvement of craniofacial LoS (i.e., the lesions tend to be concentrated in the upper face or lower face). Although facial muscles also showed varying degrees of atrophy, they were not correlated with the overall degree of soft tissue atrophy. In addition, we found that the severity of soft tissue atrophy appeared to be uncorrelated with bony tissue. This may have been due to the different ages of onset, where onset before facial skeletal maturation may lead to more severe skeletal damage. Therefore, increased attention to skeletal involvement in juvenile patients is needed, as severe atrophy of the facial bones increases the difficulty of reconstruction surgery. Further studies are needed to assess facial skeletal damage.

Clinical manifestations of craniofacial LoS with neurological involvement are usually reported as headache, seizure, and migraine. In previous studies, hyperintense or hypointense signals were found in some patients (4,28). However, in our cohort, none of these manifestations were found except for in one patient with surgically treated epilepsy, possibly due to the small sample size or the patients being in a stable state. Another limitation was

1902

Ma et al. Damage evaluation of craniofacial morphea by MRI

that the measurements were based on tissue thickness, and whether volume changes could better reflect the disease needs further investigation.

Conclusions

Our study presents a new use for MRI in evaluating craniofacial LoS, and ASTAI can be a useful and objective tool for overall craniofacial LoS evaluation. Further studies with larger sample sizes and long-term follow-ups are needed to verify our findings.

Acknowledgments

Footnote

Reporting Checklist: The authors have completed the STROBE reporting checklist. Available at https://qims.amegroups.com/article/view/10.21037/qims-23-980/rc

Conflicts of Interest: All authors have completed the ICMJE uniform disclosure form (available at https://qims.amegroups.com/article/view/10.21037/qims-23-980/coif). The authors have no conflicts of interest to declare.

Ethical Statement: The authors are accountable for all aspects of the work in ensuring that questions related to the accuracy or integrity of any part of the work are appropriately investigated and resolved. This study was approved by the Institutional Review Board of Peking Union Medical College Hospital (No. I-22PJ352) following the Declaration of Helsinki (as revised in 2013). Written informed consent forms were provided by the patients or the legal guardians for adolescent patients.

Open Access Statement: This is an Open Access article distributed in accordance with the Creative Commons Attribution-NonCommercial-NoDerivs 4.0 International License (CC BY-NC-ND 4.0), which permits the non-

References

1. Fett N, Werth VP. Update on morphea: part I. Epidemiology, clinical presentation, and pathogenesis. J Am Acad Dermatol 2011;64:217-28; quiz 229-30.
2. Creadore A, Watchmaker J, Maymone MBC, Pappas L, Lam C, Vashi NA. Cosmetic treatment in patients with autoimmune connective tissue diseases: Best practices for patients with morphea/systemic sclerosis. J Am Acad Dermatol 2020;83:315-41.
3. Ullman S, Danielsen PL, Fledelius HC, Daugaard-Jensen J, Serup J. Scleroderma en Coup de Sabre, Parry-Romberg Hemifacial Atrophy and Associated Manifestations of the Eye, the Oral Cavity and the Teeth: A Danish Follow-Up Study of 35 Patients Diagnosed between 1975 and 2015. Dermatology 2021;237:204-12.
4. Careta MF, Leite Cda C, Cresta F, Albino J, Tsunami M, Romiti R. Prospective study to evaluate the clinical and radiological outcome of patients with scleroderma of the face. Autoimmun Rev 2013;12:1064-9.
5. Kreuter A, Mitrakos G, Hofmann SC, Lehmann P, Sticherling M, Krieg T, Lahner N, Tigges C, Hunzelmann N, Moinzadeh P. Localized Scleroderma of the Head and Face Area: A Retrospective Cross-sectional Study of 96 Patients from 5 German Tertiary Referral Centres. Acta Derm Venereol 2018;98:603-5.
6. Kelsey CE, Torok KS. The Localized Scleroderma Cutaneous Assessment Tool: responsiveness to change in a pediatric clinical population. J Am Acad Dermatol 2013;69:214-20.
7. Arkachaisri T, Vilaiyuk S, Torok KS, Medsger TA Jr. Development and initial validation of the localized scleroderma skin damage index and physician global assessment of disease damage: a proof-of-concept study. Rheumatology (Oxford) 2010;49:373-81.
8. Chiu YE, Shmuylovich L, Kiguradze T, Anderson K, Sibbald C, Tollefson M, et al. Body site distribution of pediatric-onset morphea and association with extracutaneous manifestations. J Am Acad Dermatol 2021;85:38-45.
9. Abbas LF, Joseph AK, Day J, Cole NA, Hallac R, Derderian C, Jacobe HT. Measuring asymmetry in facial morphea via 3-dimensional stereophotogrammetry. J Am

Acad Dermatol 2023;88:101-8.

10. Martini G, Murray KJ, Howell KJ, Harper J, Atherton D, Woo P, Zulian F, Black CM. Juvenile-onset localized scleroderma activity detection by infrared thermography. Rheumatology (Oxford) 2002;41:1178-82.

11. Arkachaisri T, Fertig N, Pino S, Medsger TA Jr. Serum autoantibodies and their clinical associations in patients with childhood- and adult-onset linear scleroderma. A single-center study. J Rheumatol 2008;35:2439-44.

12. Wortsman X, Wortsman J, Sazunic I, Carreño L. Activity assessment in morphea using color Doppler ultrasound. J Am Acad Dermatol 2011;65:942-8.

13. Denadai R, Raposo-Amaral CA, Pinho AS, Lameiro TM, Buzzo CL, Raposo-Amaral CE. Predictors of Autologous Free Fat Graft Retention in the Management of Craniofacial Contour Deformities. Plast Reconstr Surg 2017;140:50e-61e.

14. Sator PG, Radakovic S, Schulmeister K, Hönigsmann H, Tanew A. Medium-dose is more effective than low-dose ultraviolet A1 phototherapy for localized scleroderma as shown by 20-MHz ultrasound assessment. J Am Acad Dermatol 2009;60:786-91.

15. Abbas LF, O'Brien JC, Goldman S, Pezeshk P, Chalian M, Chhabra A, Jacobe HT. A Cross-sectional Comparison of Magnetic Resonance Imaging Findings and Clinical Assessment in Patients With Morphea. JAMA Dermatol 2020;156:590-2.

16. Schanz S, Fierlbeck G, Ulmer A, Schmalzing M, Kümmerle-Deschner J, Claussen CD, Horger M. Localized scleroderma: MR findings and clinical features. Radiology 2011;260:817-24.

17. Shahidi-Dadras M, Abdollahimajd F, Jahangard R, Javinani A, Ashraf-Ganjouei A, Toossi P. Magnetic Resonance Imaging Evaluation in Patients with Linear Morphea Treated with Methotrexate and High-Dose Corticosteroid. Dermatol Res Pract 2018;2018:8391218.

18. Wang HC, Ling S, Wang X, Long X, Sun ET, Yu N, Dong R, Zeng A, Zhang H, Shu C. The Development and Initial Validation of PUMC Localized Scleroderma Facial Aesthetic Index: A Pilot Study. Aesthetic Plast Surg 2021;45:1531-9.

19. Zulian F, Culpo R, Sperotto F, Anton J, Avcin T, Baildam EM, Boros C, Chaitow J, Constantin T, Kasapcopur O, Knupp Feitosa de Oliveira S, Pilkington CA, Russo R, Toplak N, van Royen A, Saad Magalhães C, Vastert SJ, Wulffraat NM, Foeldvari I. Consensus-based recommendations for the management of juvenile localised scleroderma. Ann Rheum Dis 2019;78:1019-24.

20. Knobler R, Moinzadeh P, Hunzelmann N, Kreuter A, Cozzio A, Mouthon L, et al. European Dermatology Forum S1-guideline on the diagnosis and treatment of sclerosing diseases of the skin, Part 1: localized scleroderma, systemic sclerosis and overlap syndromes. J Eur Acad Dermatol Venereol 2017;31:1401-24.

21. Laxer RM, Zulian F. Localized scleroderma. Curr Opin Rheumatol 2006;18:606-13.

22. Liao X, Wang X, Xu Z, Guo S, Gu C, Jin Z, Su T, Chen Y, Xue H, Yang M. Assessment of facial autologous fat grafts using Dixon magnetic resonance imaging. Quant Imaging Med Surg 2022;12:2830-40.

23. Fedorov A, Beichel R, Kalpathy-Cramer J, Finet J, Fillion-Robin JC, Pujol S, Bauer C, Jennings D, Fennessy F, Sonka M, Buatti J, Aylward S, Miller JV, Pieper S, Kikinis R. 3D Slicer as an image computing platform for the Quantitative Imaging Network. Magn Reson Imaging 2012;30:1323-41.

24. Vinciguerra C, Toriello A, Nardone V, Romano D, Tartaglione S, Abate F, Landolfi A, Barone P. Temporal muscle thickness and survival in patients with amyotrophic lateral sclerosis. Neurol Res 2022;44:1006-10.

25. Mao SH, Hsieh YH, Chou PY, Shyu VB, Chen CT, Chen CH. Quantitative Determination of Zygomaticomaxillary Complex Position Based on Computed Tomographic Imaging. Ann Plast Surg 2016;76 Suppl 1:S117-20.

26. Verhelst PJ, Matthews H, Verstraete L, Van der Cruyssen F, Mulier D, Croonenborghs TM, Da Costa O, Smeets M, Fieuws S, Shaheen E, Jacobs R, Claes P, Politis C, Peeters H. Automatic 3D dense phenotyping provides reliable and accurate shape quantification of the human mandible. Sci Rep 2021;11:8532.

27. Ma X, Huang J, Chen Y, Wang X, Long X. Bony Hyperplasia Beneath Atrophic Soft Tissue: A Rare Case of En Coup de Sabre and Literature Review. Clin Cosmet Investig Dermatol 2023;16:2375-9.

28. Doolittle DA, Lehman VT, Schwartz KM, Wong-Kisiel LC, Lehman JS, Tollefson MM. CNS imaging findings associated with Parry-Romberg syndrome and en coup de sabre: correlation to dermatologic and neurologic abnormalities. Neuroradiology 2015;57:21-34.